

# Synthesis of Rare Earth (Dy and Pr) Metal Impregnated Asparagine Functionalized $\text{CoFe}_2\text{O}_4$ Nanocomposite: Two Novel, Efficient and Magnetically-Recoverable Catalysts for the Reduction of 4-nitrophenol

**Davarpanah, Jamal; Tamoradi, Taiebeh**

*Department of Chemistry, Production Technology Research Institute -ACECR, Ahvaz, I.R. IRAN*

**Karmakar, Bikash\*<sup>+</sup>**

*Department of Chemistry, Gobardanga Hindu College, 24-Parganas (North), INDIA*

**Veisi, Hojat**

*Department of Chemistry, Payame Noor University, P.O. Box 19395-4697 Tehran, I.R. IRAN*

**Gholami, Javad\*<sup>+</sup>**

*Department of Applied Chemistry, Faculty of Science, Malayer University, Malayer, I.R. IRAN*

**ABSTRACT:** *In recent times biomolecules engineered magnetically isolable nanoparticles have garnered significant attention in the nanocatalysis arena due to their outstanding features. Doping of rare earth metals over them brings further novelty to their properties. In this current work, we describe the successful synthesis of rare earth lanthanide ( $M = \text{Pr}, \text{Dy}$ ) impregnated asparagine adorned  $\text{CoFe}_2\text{O}_4$  as two novel magnetically isolable nanocomposite catalysts following a post-functionalization approach. The synthesized materials were characterized using physicochemical techniques like FT-IR, SEM, EDX, elemental mapping, and ICP-OES analyses. Subsequently, the catalytic efficiency of the materials was investigated in the reduction of 4-Nitrophenol (4-NP), as well-known carcinogenic contaminants of water. The progress of the reaction and its kinetics were monitored over UV-Vis spectroscopy. Among the two variants, Dy anchored catalyst was found to be more efficient than the Pr which led the reaction to completion in just 8 min. Kinetically, also Dy catalyst exhibited higher rate constants. This is the first report of Pr and Dy-anchored heterogeneous catalysts in the reduction of 4-NP. The current methodology is advantageous in terms of cleanliness, simple procedure, excellent yields in short reaction time, easy magnetic retrieval, and reusability of catalysts following several runs without significant change in catalytic activity.*

**KEYWORDS:** *Magnetic nanoparticle; Multiferrite; Amino acid capping; Reduction, 4-Nitrophenol.*

---

\* To whom correspondence should be addressed.

+ E-mail: [bikashkarm@gmail.com](mailto:bikashkarm@gmail.com) & [j.gholami@malayeru.ac.ir](mailto:j.gholami@malayeru.ac.ir)

1021-9986/2022/7/2222-2235

14/6.04

## INTRODUCTION

In recent days, the amalgamation of an active homogeneous catalyst with textured high-surface solid support towards stable and isolable heterogeneous systems has garnered the utmost importance in promoting green catalysis [1-3]. Simultaneously, the proper positioning and distribution of active catalytic sites onto the support through surface engineering is another significant area of research [4-7]. Magnetic NanoParticles (MNP) have evolved as an attractive support in a few decades based on their high specific surface area, biocompatibility, cost-effectiveness, easy reusability, and the presence of surface hydroxyl groups for suitable surface functionalization. Among them, the economical iron oxides and ferrite derivatives are of significant importance due to their unique electronic, chemical and magnetic features [8-16]. The spinel ferrites have the general formula  $MFe_2O_4$  where M is a bivalent transition metal atom like  $Mn^{2+}$ ,  $Fe^{2+}$ ,  $Co^{2+}$ ,  $Ni^{2+}$ ,  $Cu^{2+}$ , and  $Zn^{2+}$ . Also, M can be a mixture of these metals in multiferrites. These spinels are more stable and bear higher magnetic properties than bare  $Fe_3O_4$  with special structural designs. Out of these spinel ferrites,  $CoFe_2O_4$  acquires special attention due to its applications in different fields like sensing, catalysis, electronics, magnetism, and medicinal therapeutics [17-20]. However, owing to nanometric dimension and high surface energy, the NPs are often prone to agglomeration which reduces their catalytic activity [21-30]. This drawback is effectively circumvented by surface modification with a suitable capping agent. This also prevents the MNPs from aerial oxidation and solvation in organic solvents [31-34]. We have observed and successfully reported in our previous communications that amino acids and their analogs have good potential for functionalization over the MNPs [35-38]. They induce polar lipophilic properties over the material. In continuation of our endeavors on the catalytic applications of functionalized MNPs [35-46], we prefer to extend the applications of  $CoFe_2O_4$  with asparagine as amino acid capping agent.

Among the diverse organic transformations, the conversion of nitrophenol to aminophenol has been the most elementary and widely studied reaction. The depletion of toxic nitro compounds has a substantial impact on the environment as well as on industry. Different agrochemicals and synthetic dyes produce 4-Nitrophenol and their derivatives as important side products. These are

very harmful organo-pollutant in water and dreadful for humans and other animals affecting the central nervous system, kidneys, and liver [47-49]. These hazardous chemicals are resistant to microbial degradation and thereby safe exclusion of them has been a challenge. Among the different established methods of this transformation, the catalytic reduction has been proven to be the most efficient [50-53]. The amines so produced are relatively mild and benign. They also have widespread applications in the synthesis of drugs and pharmaceuticals, fine chemicals, agrochemicals, dyes, polymers, cosmetics, and photography [54].

In consideration of such consequences herein, we wish to report the Dysprosium (Dy) and Praseodymium (Pr) anchored asparagine functionalized magnetic  $CoFe_2O_4$  composite as a novel catalyst to explore the reduction of nitrophenols in a facile and green chemical pathway using sodium borohydride ( $NaBH_4$ ) as a hydrogen donor. The Dy and Pr catalysis in this particular reaction has not been reported yet. Interestingly, our protocol has been proven to be highly competent affording excellent yields within a very short time. Additionally, the strong magnetic core helped the catalyst for facile retrieval from the reaction flask using a magnetic stick and subsequent reuse several times without a considerable change in its efficiency. The progress of the reaction was precisely monitored over a UV-Vis spectrophotometer followed by a kinetic study over both of the catalysts.

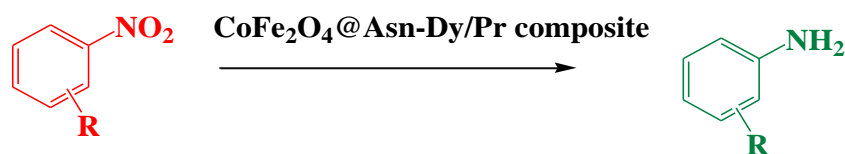
## EXPERIMENTAL SECTION

### Materials

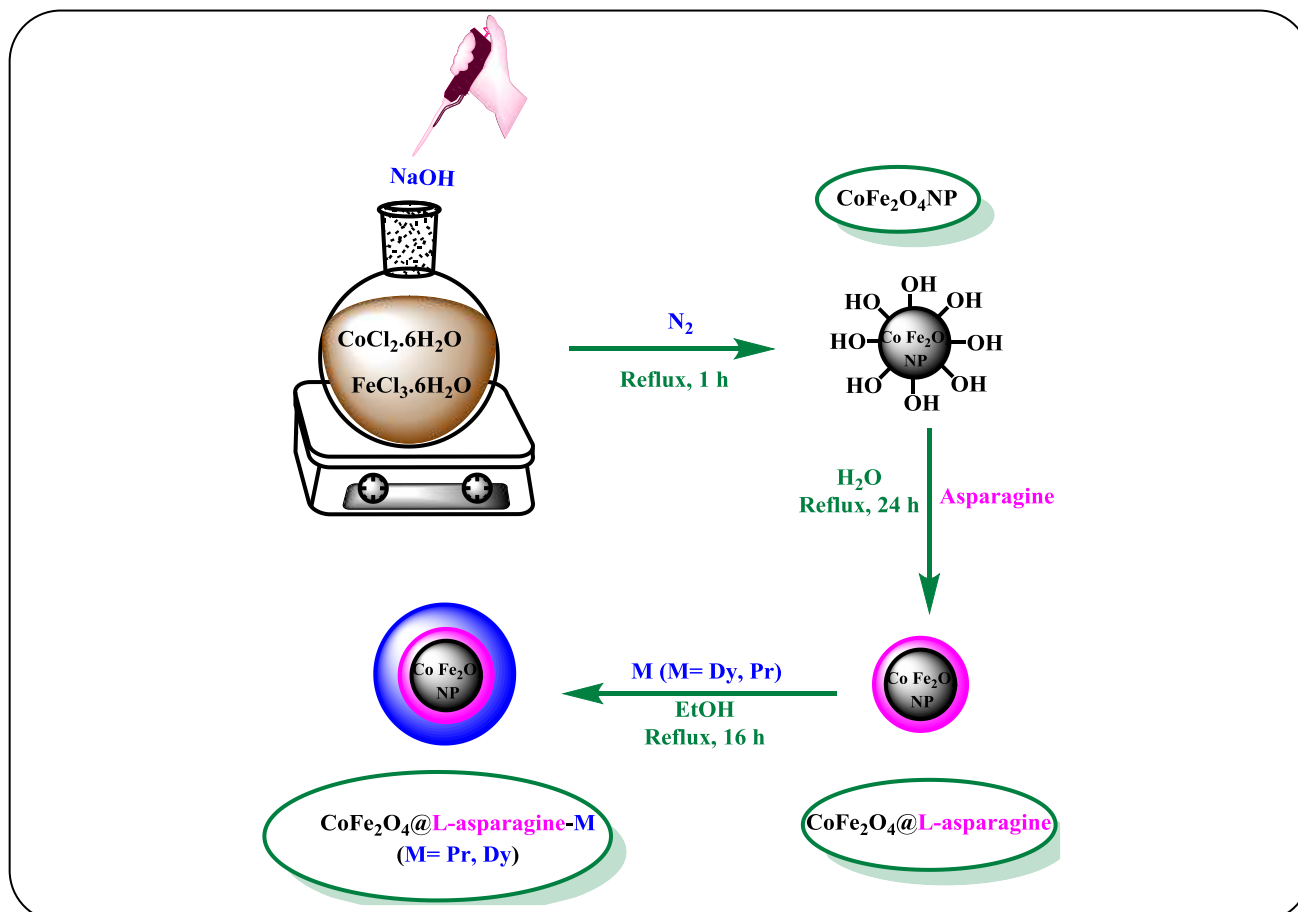
For the synthesis of catalyst  $FeCl_3 \cdot 6H_2O$ ,  $CoCl_2 \cdot 6H_2O$ , asparagine,  $Pr(NO_3)_3$  and  $Dy(NO_3)_3$  were purchased from Sigma-Aldrich. Nitrophenol and the desired solvents were purchased from Merck. All the reagents were used without further purification.

### Instrumentation

Structural morphology, particle size, and atom mapping of the catalyst were studied using a FESEM-TESCAN MIRA3 microscope equipped with EDX (TSCAN). Fourier transform infrared, FT-IR (Bruker VERTEX 80 v) was also utilized for the characterization of prepared samples. The powder XRD of the nanostructures was done using  $Co K\alpha$  radiation ( $\lambda = 1.78897 \text{ \AA}$ ) operating at 40 keV, and a cathode current of 40 Ma in the scanning range of



Scheme 1: Reduction of 4-nitrophenol over  $\text{CoFe}_2\text{O}_4@ \text{Asn-Dy/Pr}$  nanocatalyst.



Scheme 2: A schematic diagram in the synthesis of  $\text{CoFe}_2\text{O}_4@ \text{Asn-Dy/Pr}$  nanocatalyst.

$2\theta = 5$  to  $80$ . VSM measurement was recorded in a vibrating sample 244 magnetometer by a Vibrating Sample Magnetometer (VSM) MDKFD at room temperature.

#### Synthesis of $\text{CoFe}_2\text{O}_4$ nanoparticles

2.63 g of  $\text{FeCl}_3$  and 1.19 g of  $\text{CoCl}_2$  were dissolved in 50 mL of deionized water under stirring conditions. A 20 mL 15% aqueous NaOH solution was added dropwise to the mixture and the resulting solution was refluxed for 1 h. The color of the solution turned dark brown indicating the formation of the product. The products were isolated using

a bar magnet and subsequently washed several times with deionized water and ethanol. They were dried in the oven at  $60^\circ\text{C}$  overnight.

#### Synthesis of asparagine functionalized $\text{CoFe}_2\text{O}_4$ nanoparticles ( $\text{CoFe}_2\text{O}_4@ \text{Asn}$ )

1.5 g of asparagine was added to the suspensions of 1.0 g  $\text{CoFe}_2\text{O}_4$  in 30 mL double distilled water. Then, the mixture was refluxed for 24 h under stirring conditions. The obtained product was separated by an external magnet and processed previously.

### Synthesis of $\text{CoFe}_2\text{O}_4@ \text{Asn-Dy/Pr}$ nanocomposite

1.0 g of  $\text{CoFe}_2\text{O}_4@ \text{Asn}$  nanocomposite was suspended in 30 mL ethanol and 2.5 mmol of  $\text{M}(\text{NO}_3)_3$  ( $\text{M} = \text{Pr}, \text{Dy}$ ) salt was added to the suspension. The mixture was refluxed for 16 h to obtain the  $\text{CoFe}_2\text{O}_4@ \text{Asn-Dy/Pr}$  nanocatalyst. The whole process has been depicted in scheme 2.

### Catalytic reduction of 4-nitrophenol over $\text{CoFe}_2\text{O}_4@ \text{Asn-Dy/Pr}$

An aqueous solution (3.0 mL) of 4-NP of 2.5 mM concentration was added to freshly prepared  $\text{NaBH}_4$  (1.0 mL,  $2.5 \times 10^{-4}$  M) solution and stirred at room temperature. The  $\text{CoFe}_2\text{O}_4@ \text{Asn-Dy/Pr}$  catalyst (0.01 mol%) was then added to the reaction mixture. In addition to the catalyst, the reduction starts which is indicated by the gradual disappearance of the yellow color of the solution. These visible changes in the progress of the reaction were monitored by UV-Vis spectroscopy. After a requisite time, the color of the solution totally faded out and eventually became colorless due to the formation of 4-AP.

## RESULTS AND DISCUSSION

### Catalyst characterization data analysis

Physicochemical morphology and composition of the as-prepared material were thoroughly characterized using different analytical techniques like Fourier Transformed Infrared Spectroscopy (FT-IR), Scanning Electron Microscopy (SEM), Energy Dispersive X-ray (EDX) spectroscopy, and Wavelength Dispersive X-ray (WDX) spectroscopy).

Fig. 1 represents a comparative FT-IR spectrum profile of bare  $\text{CoFe}_2\text{O}_4$ ,  $\text{CoFe}_2\text{O}_4@ \text{Asn}$ ,  $\text{CoFe}_2\text{O}_4@ \text{Asn-Pr}$ , and  $\text{CoFe}_2\text{O}_4@ \text{Asn-Dy}$  (1a-1d). Fig. 1a shows the spectrum of  $\text{CoFe}_2\text{O}_4$  itself where characteristic metal-oxygen bond and hydroxyl functional group (O-H) appears in the absorption region around 580-590 and 3450-3500  $\text{cm}^{-1}$  respectively. The similarity between the following spectra reveals that the basic structure remained intact even after functionalization. The absorption peaks due to C-N and C=O stretching vibrations from asparagine moiety functionalized on  $\text{CoFe}_2\text{O}_4$  nanoparticles are observed at approximately at 1400 and 1640  $\text{cm}^{-1}$  respectively. The absorption peaks due to strong vibrations of asparagine carboxylic acid groups on the surface of  $\text{CoFe}_2\text{O}_4$  nanoparticles are observed at approximately 150-1100  $\text{cm}^{-1}$ . However, any particular characteristic peak due to attachment

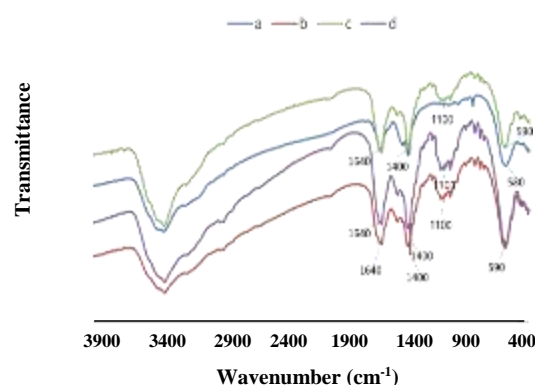


Fig. 1: FT-IR spectrum of  $\text{CoFe}_2\text{O}_4$  (a),  $\text{CoFe}_2\text{O}_4@ \text{Asn}$  (b),  $\text{CoFe}_2\text{O}_4@ \text{Asn-Pr}$  (c) and  $\text{CoFe}_2\text{O}_4@ \text{Asn-Dy}$  (d).

of Pr and Dy to the network could not be detected might be due to lower concentration.

The surface morphology, particle shape, and size were determined from SEM analysis. Fig. 2 displays the images of bare  $\text{CoFe}_2\text{O}_4$  (a),  $\text{CoFe}_2\text{O}_4@ \text{Asn-Pr}$  and  $\text{CoFe}_2\text{O}_4@ \text{Asn-Dy}$  (b-d) nanoparticles.  $\text{CoFe}_2\text{O}_4$  NP is seen to have a smooth surface. However, the surface-modified NP depicts the nanometric particles with quasi-spherical morphology. The small globules spread over the  $\text{CoFe}_2\text{O}_4$  might represent Pr and Dy NPs.

The energy-dispersive X-ray spectroscopy (EDX) analysis of both  $\text{CoFe}_2\text{O}_4@ \text{Asn-Pr}$  and  $\text{CoFe}_2\text{O}_4@ \text{Asn-Dy}$  were investigated in order to justify the exact composition of the two materials. As shown in Fig. 3a and 3b, both the profile displays Co, Fe, C, N, and O as common elements indicating the identical core structure. Pr and Dy appeared as special elements in Fig 3a and 3b respectively. The presence of C, N, and O elements confirms the amino acid attachment with the basic  $\text{CoFe}_2\text{O}_4$  core. It can be seen that the amount of Dy in the fresh catalyst and the recycled catalyst after 7 times recycling is 0.75 and 0.67 mmol/g, respectively, which indicated an insignificant amount of leaching of Dy.

The wavelength dispersive X-ray spectroscopy (WDX) or elemental mapping of the synthesized two materials  $\text{CoFe}_2\text{O}_4@ \text{Asn-Pr}$  and  $\text{CoFe}_2\text{O}_4@ \text{Asn-Dy}$  are represented in Fig. 4a and 4b respectively. In so doing, a selected area of SEM micrograph was chosen and was analyzed by X-Ray. It shows the uniform dispersion of Pr and Dy atoms in the nanocomposite. Also, the elemental analysis for the other atoms like C, N, O, Co and Fe admits homogenous dispersion throughout. The presence

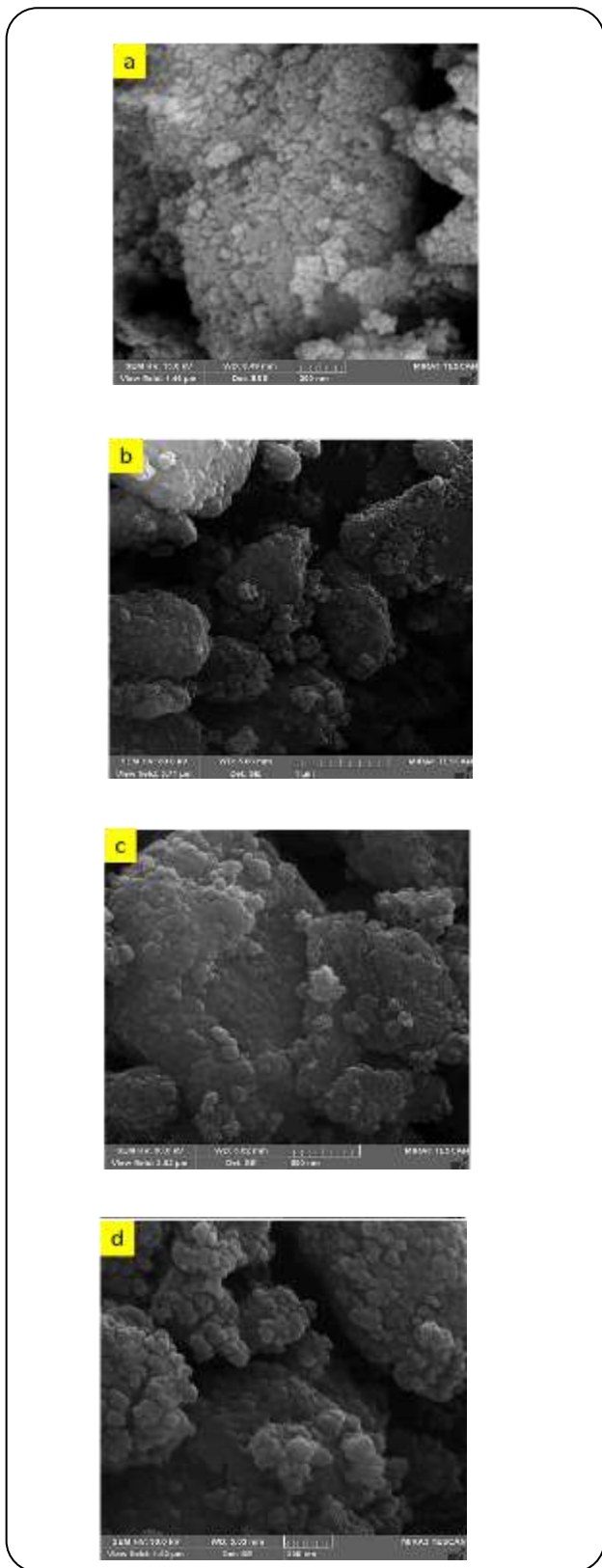


Fig. 2: SEM images of CoFe<sub>2</sub>O<sub>4</sub> (a), CoFe<sub>2</sub>O<sub>4</sub>@Asn-Dy (b, c, and d).

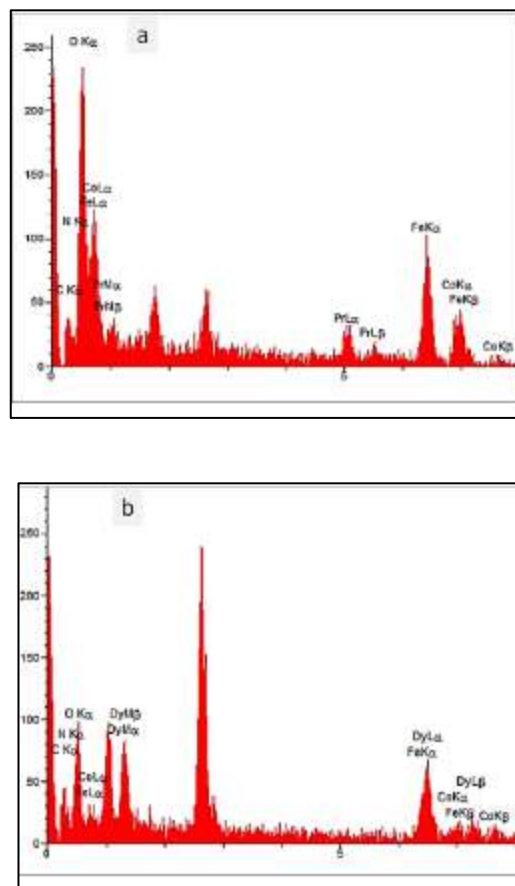


Fig. 3: EDX patterns of CoFe<sub>2</sub>O<sub>4</sub>@Asn-Pr (a) and CoFe<sub>2</sub>O<sub>4</sub>@Asn-Dy (b).

of these atoms on WDX analysis also supports the successful functionalization of asparagine moiety.

As the nanocomposite contains magnetic material in the core, the study of its magnetism through a Vibrating Sample Magnetometer (VSM) is significant. The related output for CoFe<sub>2</sub>O<sub>4</sub>@Asn-Pr is represented as a hysteresis loop, has been shown in Fig. 5. The saturation magnetization value (M<sub>s</sub>) of CoFe<sub>2</sub>O<sub>4</sub>@Asn-Pr was found to be 23.5 emu/g. It can be seen that the magnetic saturation for CoFe<sub>2</sub>O<sub>4</sub> nanoparticles is higher than the surface-modified samples which are due to the incorporation of non-magnetic Asn and rare earth metals on the surface of CoFe<sub>2</sub>O<sub>4</sub> magnetic nanoparticles [36].

The crystalline structures of fresh and 6 times reused CoFe<sub>2</sub>O<sub>4</sub>@Asn-Dy catalysts were analyzed by XRD, as presented in Fig. 6a and b respectively. The pattern reveals six characteristic sharp diffraction peaks being assigned to (2 2 0), (3 1 1), (4 0 0), (4 2 2), (5 1 1), and (4 4 0) diffraction planes of CoFe<sub>2</sub>O<sub>4</sub> inverse cubic spinel.

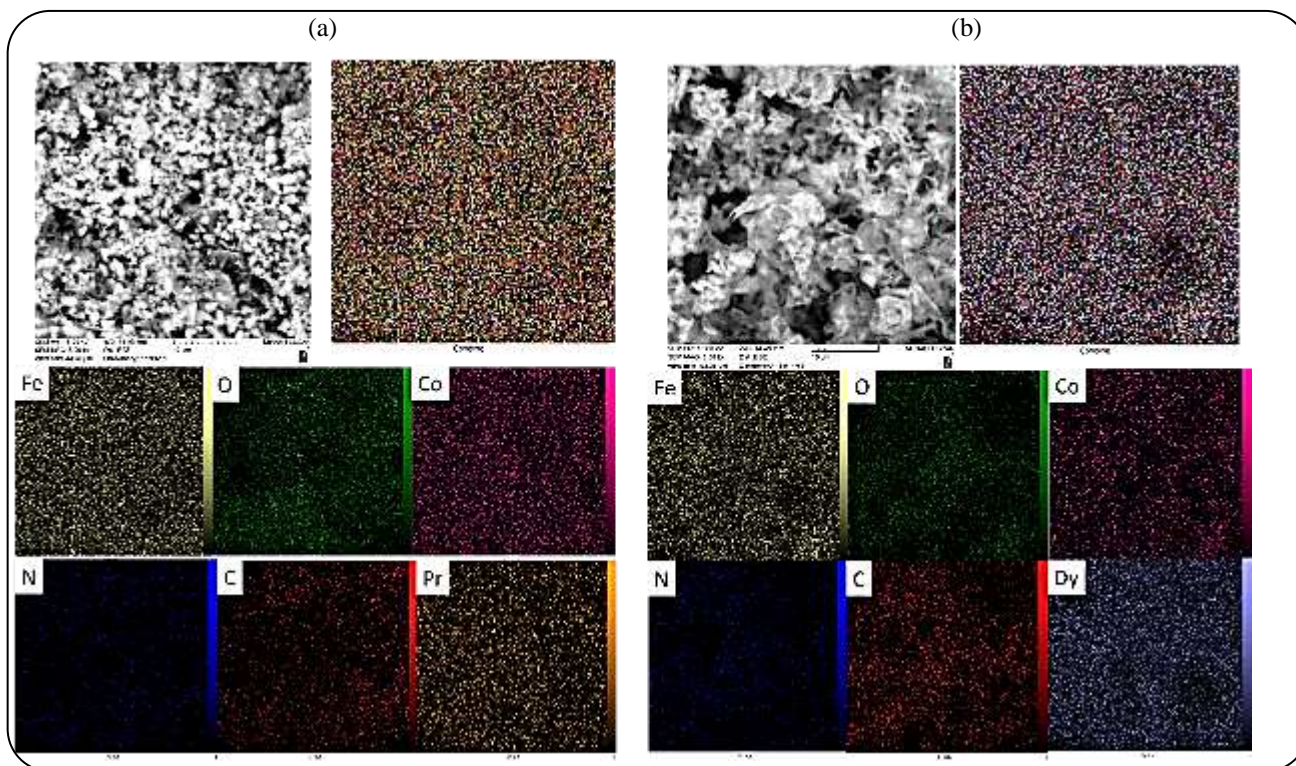


Fig. 4: X-ray atomic map analysis of CoFe<sub>2</sub>O<sub>4</sub>@Asn-Pr (a) and CoFe<sub>2</sub>O<sub>4</sub>@Asn-Dy (b).

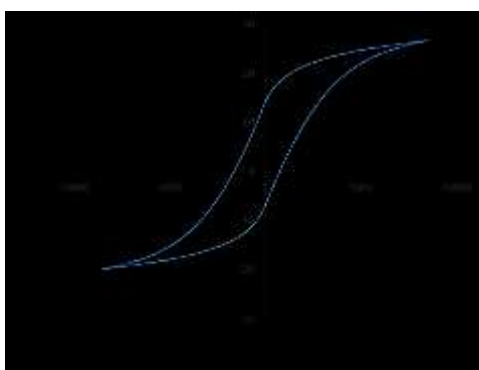


Fig. 5: VSM hysteresis loop of CoFe<sub>2</sub>O<sub>4</sub>@Asn-Pr.

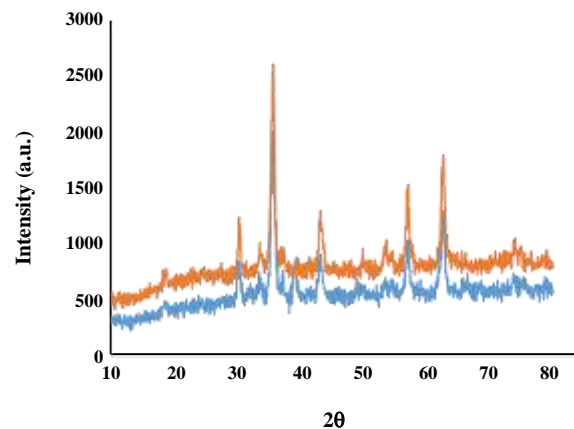


Fig. 6: XRD pattern of fresh (a) and reused (b) CoFe<sub>2</sub>O<sub>4</sub>@Asn-Dy catalyst.

It clearly displays that surface modification has not altered its core structure. In addition, the reused catalyst retains its morphology even after 6 times use.

#### Catalytic and kinetic investigation of CoFe<sub>2</sub>O<sub>4</sub>@Asn-Dy and CoFe<sub>2</sub>O<sub>4</sub>@Asn-Pr nanocomposite

After the detailed physicochemical characterizations of the surface-modified nanomagnetic catalysts, the next

endeavor was to investigate their catalytic activity. We explored the CoFe<sub>2</sub>O<sub>4</sub>@Asn-Dy/Pr catalysts in the reduction of nitrophenol using NaBH<sub>4</sub> as a reducing agent in water at room temperature. The progress of the reaction was monitored by UV-Vis spectroscopy. The output of the catalytic performances of Dy and Pr catalysts are separately documented in Fig. 7 and 8 respectively. The pale yellow colored 4-NP solution exhibited an initial

absorbance at around 320 nm. In addition  $\text{NaBH}_4$ , the color of the solution was intensified due to the formation of 4-nitrophenolate anion associated with a red shift with  $\lambda_{\text{max}}$  of 400 nm. However, no other significant change was observed except for a slight reduction of the absorption peak even, if the mixture was kept for 1h (Fig 7a). The subsequent addition of the catalyst drastically changed the scenario when the 4-NP was activated for reduction. Just after the addition of  $\text{CoFe}_2\text{O}_4@\text{Asn-Dy}$  catalyst, the  $\lambda_{\text{max}}$  value sharply started collapsing with the concurrent appearance of a new peak at 295 nm ascribed to 4-aminophenol, the concentration of which was gradually increased (Fig. 7b). As can be observed from Fig 7c, within 8 minutes the 4-NP peak gradually disappeared with the permanent formation of 4-AP. Visually, the reaction mixture became colorless, an indication of a complete reduction. However, in the case of  $\text{CoFe}_2\text{O}_4@\text{Asn-Pr}$  catalyst, the reaction was continued for a longer time (20 min) but the reduction was not fully complete. Fig. 8 revealed that the initial peak of 4-NP did not get disappear although there was an indication for the formation of 4-AP. The results certainly gratified the much better catalytic performance of Dy-loaded material as compared to Pr.

Subsequently, the kinetics of the reaction was explored utilizing the UV-Vis results. The absorbance ratio of 4-NP at different time intervals,  $A_t/A_0$ , ( $A_t$  and  $A_0$  are absorbance at  $t$  and zero time) is proportional to the ratio of corresponding concentrations  $C_t/C_0$  ( $C_t$  and  $C_0$  are the concentration of 4-NP at  $t$  and zero time). Thereby, the rate constant ( $k_c$ ) was estimated from the following rate equation:

$$dC_t/dt = -k_c C_t \quad (1)$$

On integrating this in the limit range of  $C_0$  and  $C_t$  we get,

$$\ln C_t/C_0 = \ln A_t/A_0 = -k_c t \quad (2)$$

Hence, the rate constant  $k_c$  can be determined from the slopes of the plot of  $\ln(C_t/C_0)$  vs time (s) as a function of catalyst load. Due to the higher concentration of  $\text{NaBH}_4$  as compared to the substrate, the rate constant is assumed to be independent of it. On plotting the values for  $\text{CoFe}_2\text{O}_4@\text{Asn-Pr}$  catalysis, the rate constant values were obtained as  $0.005 \text{ s}^{-1}$ ,  $0.009 \text{ s}^{-1}$ , and  $0.026 \text{ s}^{-1}$  respectively for the catalyst amount of 1, 4, and 16 mg (Fig. 9a). While performing the same analysis with  $\text{CoFe}_2\text{O}_4@\text{Asn-Dy}$  catalyst, there was a lot of differences in the nature of plots

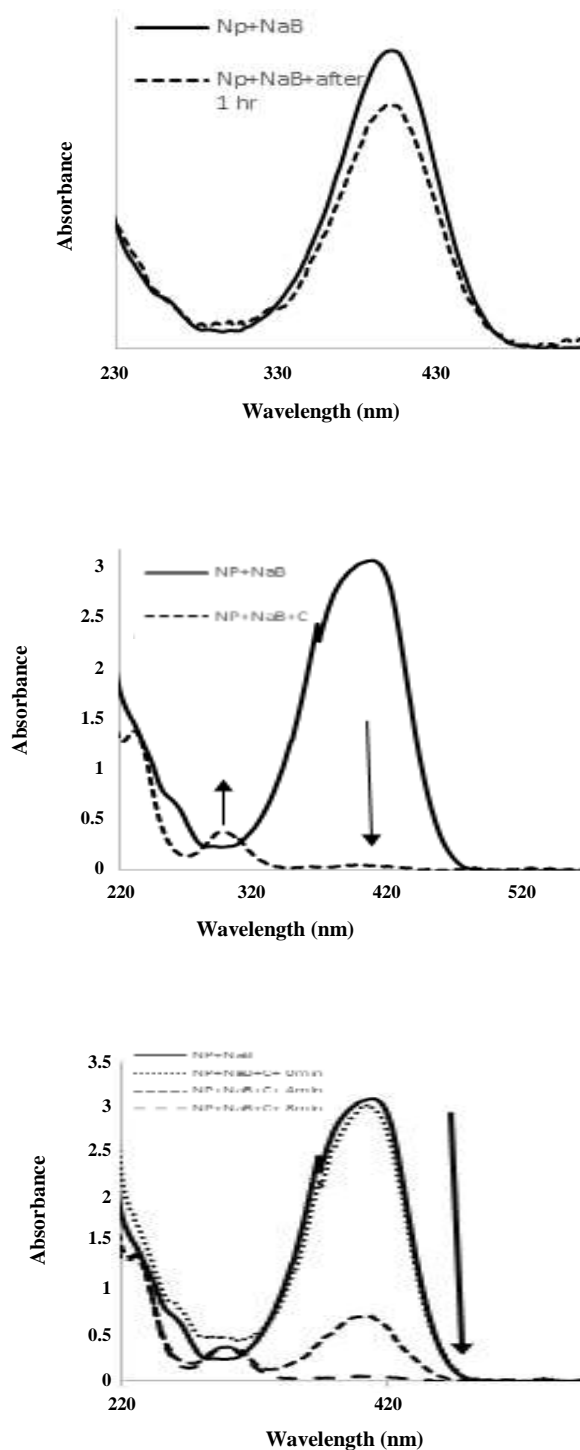


**Fig. 7:** The reduction of the 4-nitrophenol (NP) by sodium borohydride (NaB) catalyzed by  $\text{CoFe}_2\text{O}_4@\text{Asn-Dy}$ ; UV-Vis absorption spectra a) NP + NaB solution in the absence of catalyst after 1 hr, b) NP solution before and after addition of catalyst, c) the reduction catalyzed by the catalyst in the different time (min).

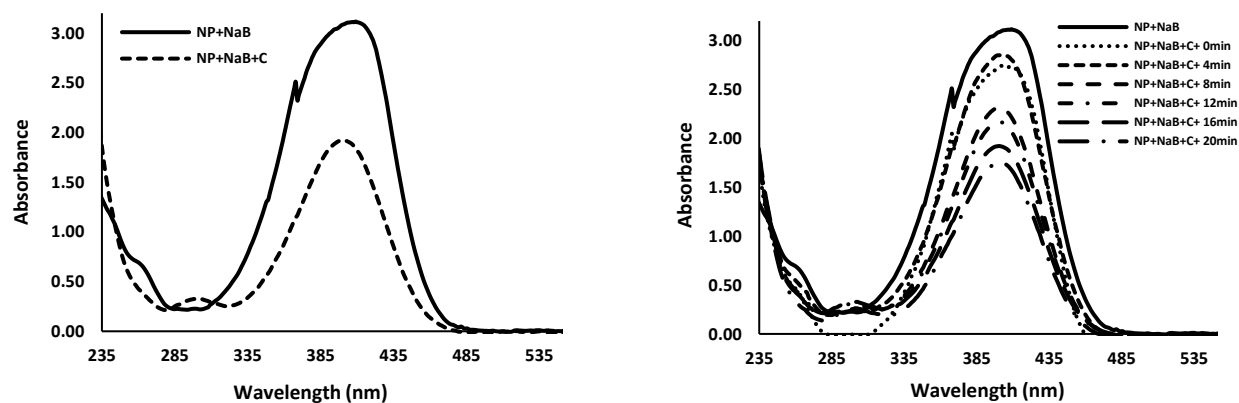


Fig. 8: The UV-Vis absorption spectra for reduction of the 4-nitrophenol (NP) using sodium borohydride (NaB) catalyzed by  $\text{CoFe}_2\text{O}_4\text{@Asn-Pr}$  NP catalyst; a) before and after addition of the catalyst, b) the reduction catalyzed by catalyst at different time (min).

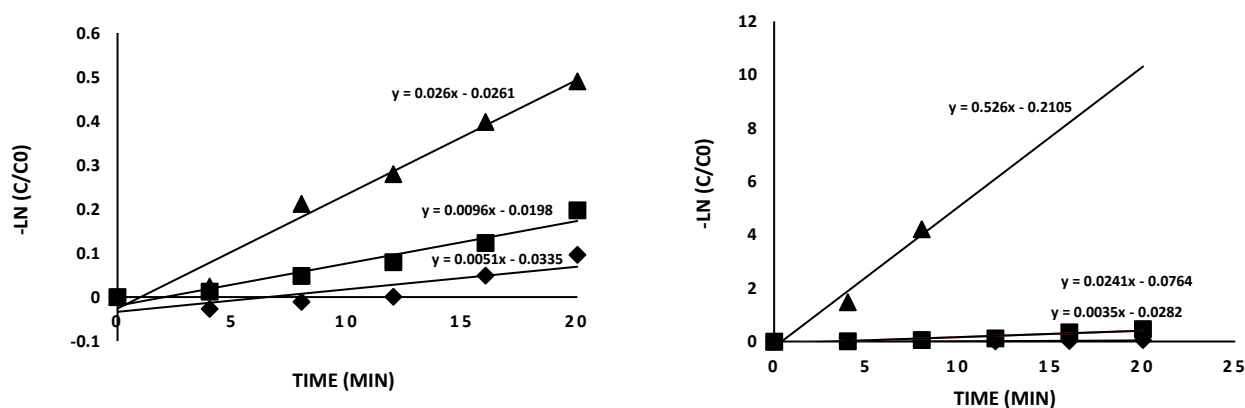


Fig. 9: Plot of  $-\ln(C_t/C_0)$  vs reaction time for the a)  $\text{CoFe}_2\text{O}_4\text{@Asn-Pr}$  and b)  $\text{CoFe}_2\text{O}_4\text{@Asn-Dy}$  catalysis.

as can be seen in Fig. 7b. The rate constants were found as 0.003, 0.024, and 0.526 at catalyst amounts of 1, 4, and 16 mg respectively. So, a catalyst amount of 16 mg resulted in the optimum with a rate constant of 0.526. Evidently, the Dy-loaded catalyst performance was much better than Pr.

#### The mechanistic study

Following literature analysis, a plausible mechanistic pathway for the  $\text{CoFe}_2\text{O}_4\text{@Asn-M}$  (Pr, Dy) catalyzed reduction of 4-NP could be explained [55, 56]. At the outset, the borohydride ions get adsorbed on the MNP exterior surface of the catalyst and subsequently release hydride ions ( $\text{H}^-$ ) to the anchored lanthanide metals. Due to strong Lewis acidity, the Ln metals form a stable metal-hydride complex. In the meantime, the 4-NP also binds to the catalyst surface. Thereafter, interfacial electron transfer occurs from hydrides to 4-NP and slowly it gets

transformed to 4-AP. However, the conversion path involves several important intermediates like nitrosophenol and hydroxylaminophenol as shown in Scheme 3. The rate of electron transfer is proportional to the conversion rate. Finally, desorption of 4-AP takes place from the catalyst surface leaving behind the catalytic site free for the new cycle.

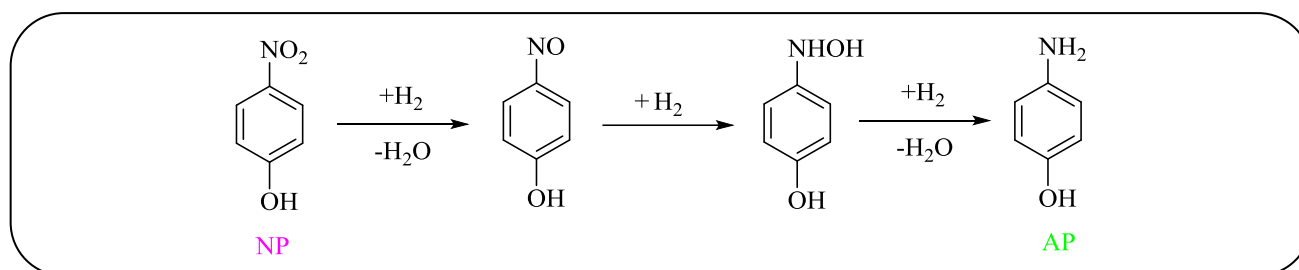
#### Study of reusability for $\text{CoFe}_2\text{O}_4\text{@Asn-Dy}$

In view of maintaining green protocols, the reusability of the catalyst is an utmost important factor. Due to the strong magnetic core, the catalyst could be easily isolated using an external magnet and recycled after drying. In the catalytic reduction of 4-NP using the catalyst  $\text{CoFe}_2\text{O}_4\text{@Asn-Dy}$ , we could reuse it up to seven times without a considerable change in its catalytic activity, thereby proving its robustness as well (Fig. 10).



**Table 1: Comparison efficiency of CoFe<sub>2</sub>O<sub>4</sub>@Asn-Dy nanocomposite with some reported methods for the reduction of 4-nitrophenol**

Entry	Catalyst (mol%)	Conditions	Time (h)	Yield (%)	Refs.
7	Rh	N <sub>2</sub> H <sub>4</sub> , EtOH, 80 °C	2.5	94	57
9	PdCu/graphene	NaBH <sub>4</sub> , EtOH:H <sub>2</sub> O (1:2), 50 °C	1.5	98	58
1	Au/MTA	NaBH <sub>4</sub> , EtOH, RT	3	90	59
3	Pd NPs/RGO	NaBH <sub>4</sub> , EtOH:H <sub>2</sub> O, 50 °C.	1.5	97	60
5	Nickel-iron mixed oxide	N <sub>2</sub> H <sub>4</sub> .H <sub>2</sub> O, propan-2-ol, Reflux	1.75	93	61
6	[Pt]@SiC <sub>6</sub>	AcOEt, H <sub>2</sub> , RT	3	99	62
4	Fe-phenanthroline/C	N <sub>2</sub> H <sub>4</sub> .H <sub>2</sub> O, THF, 100 °C	10	97	63
2	Fe <sub>3</sub> O <sub>4</sub> Ni MNPs	Glycerol, KOH, 80 °C	3.5	88	64
10	CoFe <sub>2</sub> O <sub>4</sub> @Asn-Dy	NaBH <sub>4</sub> , H <sub>2</sub> O, RT,	8 min	97	This work



**Scheme 3: The intermediate pathway from 4-NP to 4-AP.**

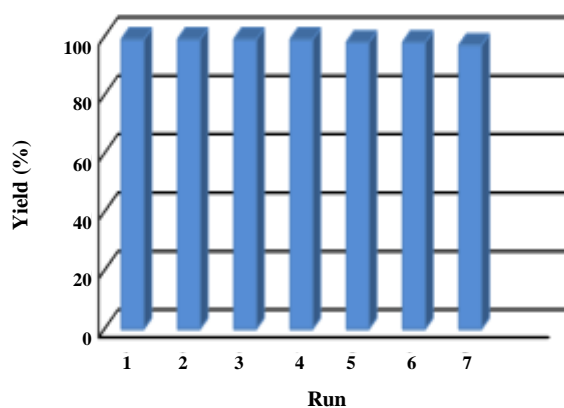


**Fig. 10: Study of reusability of CoFe<sub>2</sub>O<sub>4</sub>@Asn-Dy nanocomposite in the reduction of 4-NP.**

#### Test of heterogeneity

In order to study the heterogeneity of CoFe<sub>2</sub>O<sub>4</sub>@Asn-Dy nanocomposite, a hot filtration test was conducted in the reduction of 4-NP to 4-AP at standardized conditions. The reaction was stopped after 10 min when it was only 65% yield and the catalyst was isolated by magnetic

decantation from the reaction mixture. The catalyst-free hot filtrate was further stirred at the same conditions for an additional 10 min. Interestingly, the reaction did not proceed further within this period. This justifies that no active species has been leached out into the reaction mixture. The fact was also confirmed by ICP-OES analysis thereby approving the true heterogeneous nature of the catalyst.

#### Exclusivity of our results

To convey the uniqueness of our developed protocol, we compared our results in the reduction of 4-NP with some earlier reported methods as documented in Table 1. The CoFe<sub>2</sub>O<sub>4</sub>@Asn-Dy nanocomposite catalyst showed much superiority to others in terms of reaction time and yield.

#### CONCLUSIONS

It can be concluded that we have been able to synthesize the Pr and Dy immobilized asparagine fabricated CoFe<sub>2</sub>O<sub>4</sub> nanocomposite. The asparagine moiety acts as an effective capping agent to stabilize

the nanoparticles as well as a strong binder of the lanthanides using its polar functions to its surface. The novel material has been well characterized using analytical techniques like FT-IR, FE-SEM, EDX, WDX, and ICP-AES techniques. Both materials were engaged in the catalytic reduction of 4-Nitrophenols in presence of NaBH<sub>4</sub> as the reducing agent. The whole process was quantitatively monitored under UV-Vis spectrophotometer. We observed that the reaction proceeded hardly using NaBH<sub>4</sub> only and started immediately when the catalyst was added in combination. The nanocomposites, particularly the Dy-anchored catalyst exerted outstanding catalytic performance in the reduction of 4-NP with a high rate constant within a short period of time. Moreover, due to the strong magnetic core, the catalyst was easily retrieved using a magnet and recycled seven times almost retaining its activity constant.

#### Acknowledgments

The authors are deeply grateful to Payame Noor University for the financial support of this research project. BK thanks Gobardanga Hindu College for providing research facilities.

*Received : May. 20, 2021 ; Accepted : Aug. 23, 2021*

#### REFERENCES

- [1] Veisi H., Tamoradi T., Rashtiani A., Hemmati S., Karmakar B., Palladium Nanoparticles Anchored Polydopamine-Coated Graphene Oxide/Fe<sub>3</sub>O<sub>4</sub> Nanoparticles (GO/Fe<sub>3</sub>O<sub>4</sub>@PDA/Pd) as a Novel Recyclable Heterogeneous Catalyst in the Facile Cyanation of Haloarenes Using K<sub>4</sub>[Fe(CN)<sub>6</sub>] as Cyanide Source, *J. Indus. Chem. Eng.*, **90**: 379-388 (2020).
- [2] Munnik P., de Jongh P.E., de Jong K.P., Recent Developments in the Synthesis of Supported Catalysts, *Chem. Rev.*, **115**: 6687-6718 (2015).
- [3] van Deelen, T.W., Mejia C. H., de Jong K. P., Control of Metal-Support Interactions in Heterogeneous Catalysts to Enhance Activity and Selectivity, *Nature Catal.*, **2**: 955-970 (2019).
- [4] Liu L., Corma A., Metal Catalysts for Heterogeneous Catalysis: From Single Atoms to Nanoclusters and Nanoparticles, *Chem. Rev.*, **118**: 4981-5079 (2018).
- [5] Sudarsanam P., Zhong R., den Bosch S.V., Coman S.M., Parvulescu V.I., Sels B.F., Functionalised Heterogeneous Catalysts for Sustainable Biomass Valorization, *Chem. Soc. Rev.*, **47**: 8349-8402 (2018).
- [6] Daraie M., Tamoradi T., Heravi M.M., Karmakar B., Ce Immobilized 1H-pyrazole-3,5-dicarboxylic Acid (PDA) Modified CoFe<sub>2</sub>O<sub>4</sub>: A Potential Magnetic Nanocomposite Catalyst Towards the Synthesis of Diverse benzo[a]pyrano[2,3-c]phenazine Derivatives, *J. Molecul. Struct.*, **1245**: 131089 (2021).
- [7] Long J., Xu Y., Zhao W., Li H., Yang S., Mesoporous Silica Nanoparticles for Protein Protection and Delivery, *Front. Chem.*, **7**: 1-12 (2019).
- [8] Kudr J., Haddad Y., Richtera L., Heger Z., Cernak M., Adam V., Zitka O., Magnetic Nanoparticles: From Design and Synthesis to Real World Applications, *Nanomaterials*, **7**: 243-259 (2017).
- [9] Bhaduri K., Das B., Kumar R., Mondal S., Chatterjee S., Shah S., Bravo-Suarez J.J., Chowdhury B., Recyclable Au/SiO<sub>2</sub>-Shell/Fe<sub>3</sub>O<sub>4</sub>-Core Catalyst for the Reduction of Nitro Aromatic Compounds in Aqueous Solution, *ACS Omega.*, **4**: 4071-4081 (2019).
- [10] Veisi H., Najafi S., Hemmati S., Palladium Nanoparticles Anchored Polydopamine-Coated Graphene Oxide/Fe<sub>3</sub>O<sub>4</sub> Nanoparticles (GO/Fe<sub>3</sub>O<sub>4</sub>@PDA/Pd) as a Novel Recyclable Heterogeneous Catalyst in the Facile Cyanation of Haloarenes Using K<sub>4</sub>[Fe(CN)<sub>6</sub>] as Cyanide Source, *J. Industrial Engineer. Chem.*, **90**: 379-388 (2017).
- [11] Tamoradi T., Karmakar B., Kamalzare M., Bayat M., Kal-Koshvandi A.T., Maleki A., J. Mol. Struct., Synthesis of Eu(III) Fabricated Spinel Ferrite Based Surface Modified Hybrid Nanocomposite: Study of Catalytic Activity Towards The Facile Synthesis of Tetrahydrobenzo[B]Pyrans, *J. Molecul. Struct.*, **1219**: 128598 (2020).
- [12] Baig R.B.N., Varma R.S., Magnetically Retrievable Catalysts for Organic Synthesis, *Chem. Commun.*, **49**: 752-770 (2013).
- [13] Nematy M., Tamoradi T., Veisi H., Immobilization of Gd (III) Complex on Fe<sub>3</sub>O<sub>4</sub>: A Novel and Recyclable Catalyst for Synthesis of Tetrazole and S-S Coupling, *Polyhedron.*, **167**: 75-84 (2019).

- [14] Nasrollahzadeh M., Issaabadi Z., Sajadi S.M., Fe<sub>3</sub>O<sub>4</sub>@SiO<sub>2</sub> Nanoparticle Supported Ionic Liquid for Green Synthesis of Antibacterially Active 1-Carbamoyl-1-Phenylureas in Water, *RSC Adv.*, **8**: 27631-27644 (2018).
- [15] Narollahzadeh M., Issaabadi Z., Varma R.S., Magnetic Lignosulfonate-Supported Pd Complex: Renewable Resource-Derived Catalyst for Aqueous Suzuki–Miyaura Reaction, *ACS Omega.*, **4**: 14234–14241 (2019)
- [16] Gawande M.B., Branco P.S., Varma R.S., Nano-Magnetite (Fe<sub>3</sub>O<sub>4</sub>) as a Support for Recyclable Catalysts in the Development of Sustainable Methodologies, *Chem. Soc. Rev.*, **42**: 3371-3393 (2013).
- [17] Moghaddam F.-M., Tavakoli G., Rezvani H.R., A Copper-Free Sonogashira Reaction Using Nickel Ferrite as Catalyst in Water, *Catal. Commun.*, **60**: 82-87 (2015).
- [18] Tamoradi T., Daraie M., Heravi M.M., Karmakar B., Erbium Anchored Iminodiacetic Acid (IDA) Functionalized CoFe<sub>2</sub>O<sub>4</sub> Nano Particles: An Efficient Magnetically Isolable Nanocomposite for the Facile Synthesis of 1,8-Naphthyridines, *New J. Chem.*, **44**: 11049-11055 (2020).
- [19] Daraie M., Heravi M.M., Tamoradi T., Investigation of Photocatalytic Activity of Anchored Dysprosium and Praseodymium Complexes on CoFe<sub>2</sub>O<sub>4</sub> in Synthesis of Pyrano[2,3-d]pyrimidine Derivatives, *Chem Select.*, **4**, 10742-10747 (2019).
- [20] Tamoradi T., Veisi H., Karmakar B., Gholami J., A Competent Green Methodology for the Synthesis of Aryl Thioethers and 1H-Tetrazole over Magnetically Retrievable Novel CoFe<sub>2</sub>O<sub>4</sub>@l-Asparagine Anchored Cu, Ni Nanocatalyst, *Material Sci Engineer: C*, **107**: 110260 (2020).
- [21] Dewan A., Sarmah M., Thakur A.J., Bharali P., Bora U., Greener Biogenic Approach for the Synthesis of Palladium Nanoparticles Using Papaya Peel: An Eco-Friendly Catalyst for C–C Coupling Reaction, *ACS Omega.*, **3**: 5327–5335 (2018).
- [22] Abboud Y., Saffaj T., Chagraoui A., El Bouari A., Brouzi K., Tanane O., Ihssane B., Biosynthesis, Characterization and Antimicrobial Activity of Copper Oxide Nanoparticles (CONPs) Produced Using Brown Alga Extract (*Bifurcaria bifurcata*), *Appl. Nanosci.*, **4**: 571-576 (2014).
- [23] Sarmah M., Neog A.B., Boruah P.K., Das M.R., Bharali P., Bora U., Effect of Substrates On Catalytic Activity of Biogenic Palladium Nanoparticles in C–C Cross-Coupling Reactions, *ACS Omega.*, **4**, 3329–3340 (2019).
- [24] Dumrongrojthanath P., Thongtem T., Phuruangrat A., Thongtem S., Synthesis and Characterization of Hierarchical Multilayered Flower-Like Assemblies of Ag Doped Bi<sub>2</sub>WO<sub>6</sub> and Their Photocatalytic Activities, *Superlattices Microstruct.* **64**: 196-203 (2013).
- [25] Phuruangrat A., Maneechote A., Dumrongrojthanath P., Ekthammathat N., Thongtem S., Thongtem T., Effect of pH on Visible-Light-Driven Bi<sub>2</sub>WO<sub>6</sub> Nanostructured Catalyst Synthesized by Hydrothermal Method, *Superlattices Microstruct.*, **78**: 106-115 (2015).
- [26] Ghasemi Z., Abdi V., Sourinejad I., Green fabrication of Ag/AgCl@TiO<sub>2</sub> Superior Plasmonic Nanocomposite: Biosynthesis, Characterization and Photocatalytic Activity under Sunlight, *J Alloy Compd.*, **841**: 155593 (2020).
- [27] Moradi N., Amin M.M., Fatehizadeh A., Ghasemi Z., Degradation of UV-Filter Benzophenon-3 in Aqueous Solution Using TiO<sub>2</sub> Coated on Quartz Tubes, *J. Environ. Health Sci. Eng.*, **16**: 213-218 (2018).
- [28] Abdi V., Ghasemi Z., Sourinejad I., Comparative Study of the Ethanolic and Aqueous *Avicennia Marina* Mangrove Extracts on the Biosynthesis of AgCl@ TiO<sub>2</sub> nanocomposite, *Iran. J. Chem. Chem. Eng. (IJCCE)*, **40(5)**: 1375-1385 (2021).
- [29] Veisi H., Mohammadi L., Hemmati S., Tamoradi T., Mohammadi P., In Situ Immobilized Silver Nanoparticles on *Rubia Tinctorum* Extract-Coated Ultrasmall Iron Oxide Nanoparticles: An Efficient Nanocatalyst with Magnetic Recyclability for Synthesis of Propargylamines by A<sub>3</sub> Coupling Reaction, *ACS Omega.*, **4**: 13991–14003 (2019).
- [30] Abdi V., Sourinejad I., Yusefzadi M., Ghasemi Z., Biosynthesis of Silver Nanoparticles from the Mangrove *Rhizophora mucronata*: Its Characterization and Antibacterial Potential, *Iran. J. Sci. Technol. Trans. A Sci.*, **43**: 2163-2171 (2019).

- [31] Farzad E., Veisi H., Fe<sub>3</sub>O<sub>4</sub>/SiO<sub>2</sub> Nanoparticles Coated with Polydopamine as a Novel Magnetite Reductant and Stabilizer Sorbent for Palladium Ions: Synthetic Application of Fe<sub>3</sub>O<sub>4</sub>/SiO<sub>2</sub>@PDA/Pd for Reduction of 4-Nitrophenol and Suzuki reactions, *J. Indus. Eng. Chem.*, **60**: 114-124 (2018).
- [32] Sharma R.K., Dutta S., Sharma S., Zboril R., Varma R.S., Gawande M.B., Fe<sub>3</sub>O<sub>4</sub> (iron oxide)-supported Nanocatalysts: Synthesis, Characterization and Applications in Coupling Reactions, *Green Chem.*, **18**: 3184-3209 (2016)
- [33] Wang D., Astruc D., Fast-Growing Field of Magnetically Recyclable Nanocatalysts, *Chem. Rev.*, **114**: 6949-6985 (2014).
- [34] Abu-Rezig R., Alper H., Wang D., Post M.L., Metal Supported on Dendronized Magnetic Nanoparticles: Highly Selective Hydroformylation Catalysts, *J. Am. Chem. Soc.*, **128**: 5279-5282 (2006).
- [35] Tamoradi T., Veisi H., Karmakar B., Pd Nanoparticle Fabricated Tetrahydroharman-3-carboxylic Acid Analog Immobilized CoFe<sub>2</sub>O<sub>4</sub> Catalyzed Fast and Expedient C–C Cross and C–S Coupling, *Chemistry Select.*, **4**: 10953-10959 (2019).
- [36] Tamoradi T., Veisi H., Karmakar B., Gholami, J. Preparation, Structural Characterization, and Catalytic Performance of Green Synthesized Cu/Fe<sub>3</sub>O<sub>4</sub> Nanocomposite as Recyclable Nanocatalyst for Synthesis of Pyrano[3,2-C]Chromene Derivatives, *Mater Sci Eng C.*, **107**: 110260 (2020).
- [37] Tamoradi T., Taheri A., Vahedi S., Ghadermaji M., Gd (III) and Tb (III) Immobilized Tryptophan Functionalized Magnetic Nanoparticles for Eco-Friendly Oxidation Reactions, *Solid State Sci.*, **97**: 105981 (2019).
- [38] Tamoradi T., Ghorbani-Choghamarani A., Ghadermazi M., CoFe<sub>2</sub>O<sub>4</sub>@glycine-M (M= Pr, Tb and Yb): Three Green, Novel, Efficient and Magnetically-Recoverable Nanocatalysts for Synthesis of 5-substituted 1H-tetrazoles and Oxidation of Sulfides in Green Condition, *Solid State Sci.*, **88**: 81-94 (2019).
- [39] Veisi H., Tamoradi T., Karmakar B., Mohammadi P., Hemmati S., In Situ Biogenic Synthesis of Pd Nanoparticles over Reduced Graphene Oxide by Using a Plant Extract (*Thymra spicata*) and Its Catalytic Evaluation Towards Cyanation of Aryl Halides, *Mater Sci Eng C.*, **104**: 109919 (2019).
- [40] Tamoradi T., Mousavi S.M., Mohammadi M., Praseodymium(iii) Anchored on CoFe<sub>2</sub>O<sub>4</sub> MNPs: An Efficient Heterogeneous Magnetic Nanocatalyst for One-Pot, Multi-Component Domino Synthesis of Polyhydroquinoline and 2,3-dihydroquinazolin-4(1H)-one Derivatives, *New J. Chem.*, **44**: 3012-3020 (2020).
- [41] Veisi H., Moradi S.B., Saljooqi A., Safarimehr P., Silver Nanoparticle-Decorated on Tannic Acid-Modified Magnetite Nanoparticles (Fe<sub>3</sub>O<sub>4</sub>@TA/Ag) for Highly Active Catalytic Reduction of 4-Nitrophenol, Rhodamine B and Methylene Blue, *Mat. Sci. Eng. C.*, **100**: 445-452 (2019)
- [42] Veisi H., Sarachegol P., Hemmati S., Palladium(II) Anchored On Polydopamine Coated-Magnetic Nanoparticles (Fe<sub>3</sub>O<sub>4</sub>@PDA@Pd(II)): A Heterogeneous and Core–Shell Nanocatalyst in Buchwald–Hartwig C–N Cross Coupling Reactions, *Polyhedron.*, **156**: 64-71 (2018).
- [43] Tamoradi T., Ghorbani-Choghamarani A., Ghadermazi M., Fe<sub>3</sub>O<sub>4</sub>-adenine–Zn: A Novel, Green, and Magnetically Recoverable Catalyst for the Synthesis of 5-Substituted Tetrazoles and Oxidation of Sulfur Containing Compounds, *New J. Chem.*, **41**: 11714-11721 (2017).
- [44] Tamoradi T., Mehraban Esfandiari B., Ghadermaji M., Ghorbani-Choghamarani A., Immobilization of a Nickel Complex onto Functionalized Fe<sub>3</sub>O<sub>4</sub> nanoparticles: A Green and Recyclable Catalyst for Synthesis of 5-Substituted 1H-Tetrazoles and Oxidation Reactions, *Res. Chem. Intermed.*, **44**: 1363-1380 (2018).
- [45] Veisi H., Taheri S., Hemmati S., Preparation of Polydopamine Sulfamic Acid-Functionalized Magnetic Fe<sub>3</sub>O<sub>4</sub> Nanoparticles with a Core/Shell Nanostructure as Heterogeneous and Recyclable Nanocatalysts for the Acetylation of Alcohols, Phenols, Amines and Thiols under Solvent-Free Conditions, *Green Chem.*, **18**: 6337-6348 (2016).
- [46] Veisi H., Pirhayati M., Kakanejadifard A., Mohammadi P., Abdi M.R., Gholami J., Hemmati S., In Situ Green Synthesis of Pd Nanoparticles on Tannic Acid-Modified Magnetite Nanoparticles as a Green Reductant and Stabilizer Agent: Its Application as a Recyclable Nanocatalyst (Fe<sub>3</sub>O<sub>4</sub>@TA/Pd) for Reduction of 4-Nitrophenol and Suzuki Reactions, *Chemistry Select.*, **3**: 1820-1826 (2018).

- [47] Naseem K., Begum R., Farooqi Z.H., Catalytic Reduction of 2-nitroaniline: A Review, *Environ. Sci. Pollut. Res.* **24**: 6446 (2017)
- [48] Atarod M., Nasrollahzadeh M., Sajadi S.M., Green synthesis of Pd/RGO/Fe<sub>3</sub>O<sub>4</sub> Nanocomposite Using Withania Coagulans Leaf Extract and its Application as Magnetically Separable and Reusable Catalyst for the Reduction of 4-Nitrophenol, *J. Colloid Interface Sci.*, **465**, 249-258 (2016).
- [49] Nasrollahzadeh M., Issaabadi Z., Safari R., Synthesis, Characterization and Application of Fe<sub>3</sub>O<sub>4</sub>@SiO<sub>2</sub> Nanoparticles Supported Palladium(II) Complex as a Magnetically Catalyst for the Reduction of 2,4-Dinitrophenylhydrazine, 4-Nitrophenol and Chromium(VI): A Combined Theoretical (DFT) and Experimental Study, *Sep. Purif. Technol.*, **209**: 136-144 (2019).
- [50] Baran T., Biosynthesis of Highly Retrievable Magnetic Palladium Nanoparticles Stabilized on Bio-Composite for Production of Various Biaryl Compounds and Catalytic Reduction of 4-Nitrophenol, *Catal. Lett.*, **149**: 1721-1729 (2019).
- [51] Farzad E., Veisi H., Fe<sub>3</sub>O<sub>4</sub>/SiO<sub>2</sub> Nanoparticles Coated with Polydopamine as a Novel Magnetite Reductant and Stabilizer Sorbent for Palladium Ions: Synthetic Application of Fe<sub>3</sub>O<sub>4</sub>/SiO<sub>2</sub>@PDA/Pd for Reduction of 4-Nitrophenol and Suzuki Reactions, *J. Ind. Eng. Chem.* **60**: 114-124 (2018).
- [52] Veisi H., Ozturk T., Karmakar B., Tamoradi T., Hemmati S., In Situ Decorated Pd NPs on Chitosan-Encapsulated Fe<sub>3</sub>O<sub>4</sub>/SiO<sub>2</sub>-NH<sub>2</sub> as Magnetic Catalyst in Suzuki-Miyaura Coupling and 4-Nitrophenol Reduction, *Carbohydr. Polym.* **35**: 115966 (2020).
- [53] Chang Y.C., Chen D.H., Catalytic Reduction of 4-Nitrophenol by Magnetically Recoverable Au Nanocatalyst, *J. Hazard. Mater.*, **165**: 664-669 (2020).
- [54] Ayad M.M., Amer W.A., Kotp M.G., Magnetic Polyaniline-Chitosan Nanocomposite Decorated with Palladium Nanoparticles for Enhanced Catalytic Reduction of 4-Nitrophenol, *Mol. Catal.*, **439**: 72-80 (2017).
- [55] Abay A.K., Chen X., Kuo D.H., Highly Efficient Noble Metal Free Copper Nickel Oxysulfide Nanoparticles for Catalytic Reduction of 4-Nitrophenol, Methyl Blue, and Rhodamine-B Organic Pollutants, *New J. Chem.*, **41**: 5628-5638 (2017).
- [56] Wu G., Liu X., Zhou P., Wang L., Hegazy M., Huang X., Huang Y., A Facile Approach for the Reduction of 4-Nitrophenol and Degradation of Congo Red Using Gold Nanoparticles or Laccase Decorated Hybrid Inorganic Nanoparticles/Polymer-Biomacromolecules Vesicles, *Mat. Sci. Eng. C.*, **94**: 524-533 (2019).
- [57] Shokouhimehr M., Lee J. E., Han S. I., Hyeon T., Magnetically Recyclable Hollow Nanocomposite Catalysts for Heterogeneous Reduction of Nitroarenes and Suzuki Reactions, *Chem. Commun.*, **49**: 4779-4781 (2013).
- [58] Feng Y.-S., Ma J.-J., Kang Y.-M., Xu H.-J., PdCu Nanoparticles Supported on Graphene: An Efficient and Recyclable Catalyst for Reduction of Nitroarenes, *Tetrahedron*, **70**: 6100-6105 (2014).
- [59] Fountoulaki S., Daikopoulou V., Gkizis P.L., Tamiolakis I., Armatas G.S., Lykakis I. N., Mechanistic Studies of the Reduction of Nitroarenes by NaBH<sub>4</sub> or Hydrosilanes Catalyzed by Supported Gold Nanoparticles, *ACS Catal.*, **4**: 3504 (2014).
- [60] Nasrollahzadeh M., Sajadi S.M., Rostami-Vartooni A., Alizadeh M., Bagherzadeh M., Green Synthesis of the Pd Nanoparticles Supported on Reduced Graphene Oxide Using Barberry Fruit Extract and its Application as a Recyclable and Heterogeneous Catalyst for the Reduction of Nitroarenes, *J. Colloid Interf. Sci.* **466**, 360-368 (2016).
- [61] Shi Q., Lu R., Lu L., Fu X., Zhao D., Efficient Reduction of Nitroarenes over Nickel-Iron Mixed Oxide Catalyst Prepared from a Nickel-Iron Hydrotalcite Precursor, *Adv. Synth. Catal.*, **349**: 1877-1881 (2007).
- [62] Motoyama Y., Kamo K., Nagash H., Catalysis in polysiloxane Gels: Platinum-Catalyzed Hydrosilylation of Polymethylhydrosiloxane Leading to Reusable Catalysts for Reduction of Nitroarenes, *Org. Lett.*, **11**: 1345-1348 (2009).
- [63] Jagadeesh R.V., Wienhofer G., Westerhaus F.A., Surkus A.-E., Pohl M.-M., Junge H., Junge K., Beller M., Efficient and Highly Selective Iron-Catalyzed Reduction of Nitroarenes, *Chem. Commun.*, **47**: 10972-10974 (2011).

- [64] Gawande M.B., Rathi A.K., Branco P.S., Nogueira I. D., Velhinho A., Shrikhande J.J., Indulkar U.U., Jayaram R.V., Ghumman C.A.A., Bundaleski N., Teodoro O.M.N.D., Regio- and Chemoselective Reduction of Nitroarenes and Carbonyl Compounds over Recyclable Magnetic FerriteNickel Nanoparticles ( $\text{Fe}_3\text{O}_4\text{Ni}$ ) by Using Glycerol as a Hydrogen Source, *Chem. Eur. J.*, **18**: 12628 (2012).